MHD Generator Performance Analyses for the Advanced Power Train Study

Carlson C. P. Pian* and Finn A. Hals†
Avco Everett Research Laboratory, Inc., Everett, Massachusetts

Comparative analyses of different magnetohydrodynamic (MHD) power train designs for early commercial MHD powerplants were performed for plant sizes of 200, 500, and 1000 MW_e. The work was conducted as part of a program to formulate an MHD Advanced Power Train development plan. This paper presents the results of the MHD generator design and topping-cycle performance analyses. All of the MHD generator designs were based on burning of coal with oxygen-enriched air preheated to 922 K.

I. Introduction

COMPARATIVE analyses of different MHD generator designs were performed for early commercial MHD powerplant applications. Powerplant sizes of nominal 200, 500, and 1000 MW total electrical output were considered. The work reported herein was conducted as part of the first phase of a planned three-phase program to formulate an MHD Advanced Power Train (APT) development plan. This paper presents the results of the MHD generator design and topping-cycle performance analyses. The bottoming plant analyses and the overall powerplant designs and economics are described in Ref. 1.

The MHD generators considered in this study were all designed to operate with preheated (922 K) oxygen-enriched air (30 to 36 molar percent oxygen) and Montana Rosebud coal dried to 5% by mass moisture content. Fuel-rich conditions were used in the MHD combustion process for NO_x emission control with an oxidizer/fuel equivalence ratio of 0.9. The seed concentration was 1% potassium by weight of the total combustion gas.

Sensitivities of the MHD generator performance to powerplant size (thermal input), oxygen enrichment level, channel length, Mach number, diffuser pressure recovery coefficient, magnetic field strength, and other factors were investigated. These sensitivity analyses were conducted in a systematic manner so that one can compare the true performance potential of the MHD generator designs between the various selected design conditions. Thus, if a design parameter was varied during the parametric analysis, the operating conditions of the MHD generator were also varied in such a manner that optimum performance was always obtained from the MHD topping cycle. The methodology and results of the generator design performance analyses are presented in Secs. II and III, respectively.

Based on these MHD generator and topping-cycle performance studies, together with the results from the overall plant performance and cost-of-electricity analyses of Ref. 1, a generator design was selected for each of the three plant sizes. Table 1 summarizes the important design data for the three generators selected. The generators for the 200 and 500 MW_e plants are of supersonic designs. Only subsonic generator designs were investigated for the largest plant size and one of these subsonic designs was selected for the 1000 MW_e plant. In these generator designs, all of the important electrical and gasdynamic parameters have been limited to values which are reasonable projections of results obtained from experimental MHD generators.

Some calculations were also carried out to investigate the part-load operating characteristics of the supersonic generator selected for the 200 MW_e plant. The results of these analyses are presented in Sec. IV. The preliminary diagonal-loading networks developed for the three selected generator designs are described in Sec. V.

II. Calculational Approach and Methodology

The MHD generator performance has been calculated for the three different plant sizes using the AERL MHD4 computer code. This generator model is based on a coupled core flow-integral boundary-layer formulation. The Joule dissipation effects in the electrode wall boundary layers and the possibility of velocity overshoots in the sidewall boundary layers are included in the analyses of the turbulent boundary layers. The detailed descriptions of MHD4 can be found in Ref. 2.

The thermochemical, transport, and electrical properties of the MHD combustion plasma are computed using the AERL-modified NASA Chemical Equilibrium Code.[3] These properties are also calculated by using the latest available data for electron affinities and collisional cross sections.[4]

The calculational procedure used to determine the operating conditons of the MHD generator is briefly described below. This procedure is adopted to ensure that the generator design will produce the maximum power output consistent with a set of prescribed generator constraints and consistent with optimizing the performance of the MHD topping cycle.

In general, several sets of calculations must be carried out at each parametric design point in order to define the generator design and operating conditions. A parametric point is taken here to be any given combination of generator mass flux, oxygen enrichment level, channel length, Mach number, etc. In the preliminary set of generator calculations, one seeks a magnetic field distribution that would yield the maximum MHD power output while satisfying a prescribed set of generator constraints. The limiting values of the electrical operating parameters of the MHD generator are shown in Table 2. These values are selected based on the experience gained from experimental long duration channel operations. A maximum peak magnetic field intensity of 6 T was assumed for subsonic channel operation; this was reduced to 4.5 T for supersonic operation.

In these preliminary calculations, the maximum performance is obtained by adjusting the magnetic field at each streamwise location such that the generator operates at the

Presented as Paper 84-0154 at the AIAA 22nd Aerospace Sciences Meeting, Reno, Nev., Jan. 9-12, 1984; received March 3, 1984; revision received Sept. 5, 1984.

*Principal Research Engineer, Energy Technology Office. Member AIAA.

†Principal Research Engineer, Energy Technology Office.

Table 1 Summary of generator design and performance data for the three recommended plants

Plant size	~200	~500	~1000
O_2 Enrichment, molar percent	32	32	32
Channel length, m	10	16	18
Mach No.	1.2	1.2	0.885
Pressure ratio	5.19	6.48	7.26
Load parameter	0.7109	0.7400	0.7807
P_{MHD}, MW_e	84.85	230.22	502.08
P^a_{net}, MW_e	51.90	149.54	343.75
Q_{wall}, MW_{th}	21.37	47.36	77.20
Maximum E_{yc}, kV/m	3.81	3.83	3.98
Maximum E_{xc}, kV/m	2.63	2.17	1.85
Maximum J_{yc}, A/cm^2	0.77	0.74	0.84
V_{Hall}, kV	22.3	29.4	28.22
Maximum β	3.94	3.98	3.91
Maximum B, T	4.5	4.5	6.0
Maximum q_{wall}, W/cm^2	314.0	353.0	406.5
Power density, MW_e/m^3	9.62	7.71	7.62
η^b_{EE}, %	16.32	19.81	23.52
η^c_{MHD}, %	9.98	12.87	16.10
η^d_{isen}, %	60.08	64.62	72.45

[a] $P_{net} = P_{MHD} - P_{comp} - P_{O_2}$, P_{comp} = cycle compressor power, P_{O_2} = O_2 - plant compressor power. [b] $\eta_{EE} = P_{MHD}/Q_{in}$, Q_{in} = coal thermal input. [c] $\eta_{MHD} = P_{net}/Q_{in}$. [d] $\eta_{isen} \simeq P_{MHD}/\Delta H_{isen}$.

Table 2 Electrical and magnetic constraints used in the APT generator design

Maximum transverse field, $E_{ycrit} = 4$ kV/m
Maximum axial field, $E_{xcrit} = 2.5$-3.0 kV/m
Maximum transverse current density, $J_{ycrit} = 1$ A/cm^2
Maximum hall parameter, $\beta_{crit} = 4$
Maximum magnetic intensity
$B_{max} = 6$ T for subsonic channel design
$= 4.5$ T for supersonic channel design

most limiting of the stress levels listed in Table 2. A theoretical optimum magnetic field distribution can be defined in this manner, an example of which is shown in Fig. 1, which applies to a 12-m subsonic generator design intended for the 200 MW_e powerplant operating at 32% oxygen enrichment. The combustor pressure is 5.71 atm and the mass flow rate equals 120.7 kg/s. The generator has a constant load parameter, $K_{ext} = 0.7425$. For this example, the $E_y = 4$ kV/m condition predominates over a large portion of the generator. The Hall parameter, $\beta = 4$ condition prevails beyond $x = 9$ m, thus causing the drop in the magnetic field profile. The theoretical magnetic field distributions obtained in this fashion are then used to determine more realistic B-field profiles which are utilized in the ensuing channel calculations.

Typical results of subsequent calculations with the modified magnetic field distribution are shown in Fig. 2. Here, the magnetic field profile was specified in the calculations and the value of the load parameter was adjusted iteratively in the solution procedure until the desired length and exit pressure were obtained. Since arrangements were made in the preliminary calculations to satisfy the prescribed constraints by tapering the magnetic field, those same constraints remain satisfied throughout the MHD channel.

In order to determine the optimum MHD power train operating condition for each parametric case investigated, the above procedure must be carried out at several different values of burner pressure. The resulting gross generator power output as a function of burner pressure can be seen in

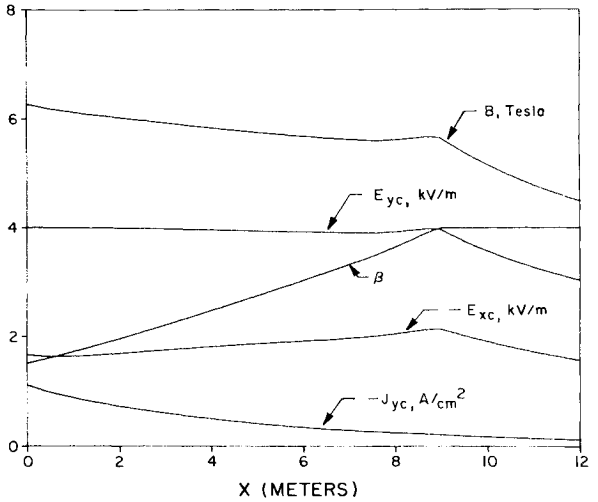

Fig. 1 Streamwise distributions of B-field, β, E_{xc}, E_{yc}, and J_{yc}. Plant size = 200 MW_e, $P_B = 5.71$ atm, $\dot{m} = 120.7$ kg/s, 32% oxygen enrichment, $K_{ext} = 0.7425$, Mach number (inlet) = 0.885.

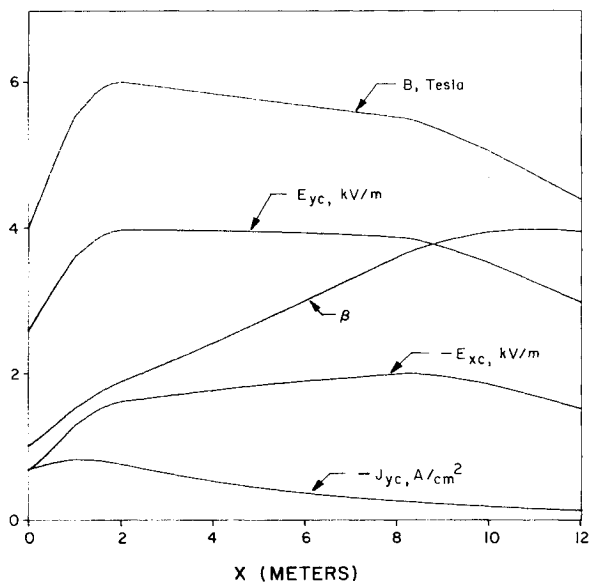

Fig. 2 Streamwise distributions of B-field, β, E_{xc}, E_{yc}, and J_{yc}. $P_B = 5.71$ atm, $K_{ext} = 0.7433$. Other conditions same as in Fig. 1.

Fig. 3a. The values of the corresponding load factor are also noted along the curve. The net power output from the topping cycle, $(P_{MHD} - P_{comp} - P_{02})$, vs the burner pressure is shown in Fig. 3b. P_{comp}, the required oxidant compressor power, is calculated assuming a compressor polytropic efficiency of 0.898 and compressor inlet condition of 289 K and 1 atm. P_{02} is the required air separation work. It is computed based on a specific power consumption of 774 kW-s per kilogram of pure equivalent oxygen. As can be seen in Fig. 3a, the gross MHD power increases with increasing burner pressure. For a given channel length (in this case, 12 m), this trend continues to still higher pressures (and lower values of K_{ext}) until a pressure is reached for which the generator cannot operate without exceeding the specified electrical and magnet constraints. However, this maximum gross power output situation is not the optimum operating condition for the powerplant, since the increased MHD power output at higher burner pressure is obtained at the expense of higher compressor work. The most desirable operating combustor pressure is at the maximum of the net power curve of Fig. 3b.

The above procedure to determine the maximum net power condition must be evaluated for each parametric point. The resulting generator design data and corresponding topping-

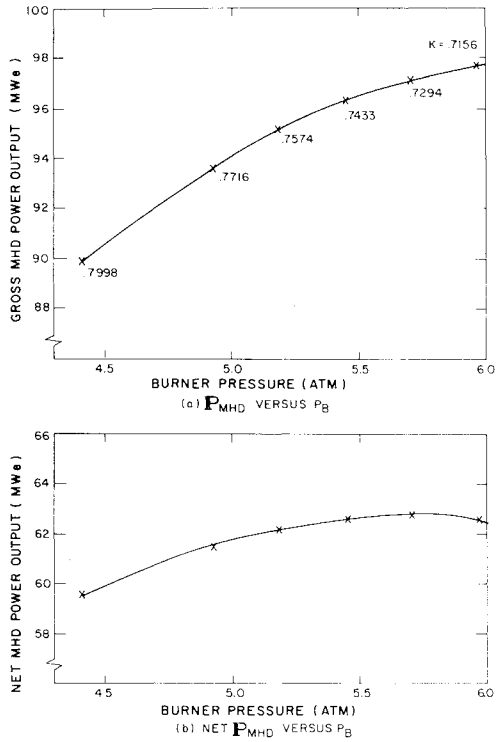

Fig. 3 Typical MHD power and net MHD power variations. Plant size = 200 MW_e, generator length = 12 m, 32% oxygen enrichment, Mach number (inlet) = 0.885.

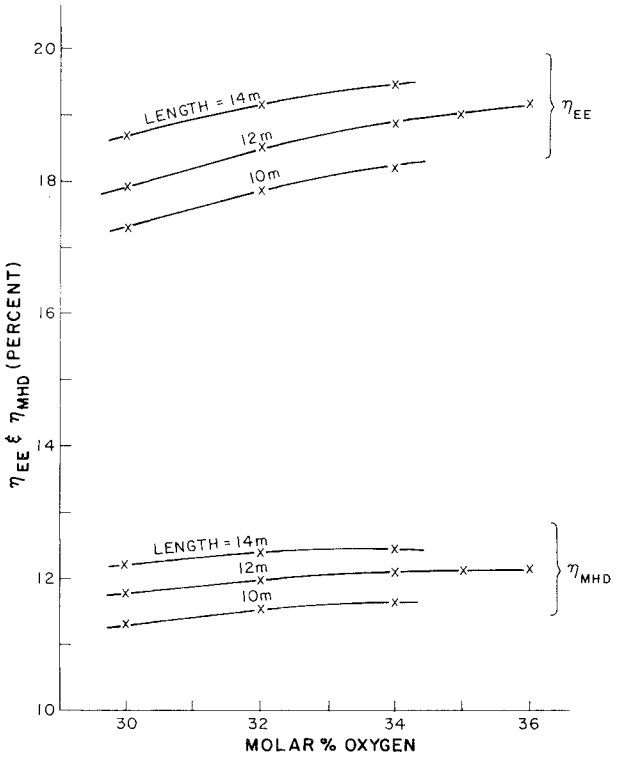

Fig. 4 Variations of η_{EE} and η_{MHD} with oxygen enrichment and length, 200 MW_e plant sizes, subsonic.

plant operating conditions are then used in the overall plant performance and cost analyses reported in Ref. 1. Unless stated otherwise, all of the MHD generator design and performance data presented in this paper are those for the maximum P_{net} conditions.

Although the baseload MHD generators might very well have multiple diagonal loads, the generator analyses for the parametric investigation are Faraday loaded. The results of these Faraday generators are used to select the optimal operating conditions (e.g., oxygen enrichment level, channel Mach number, etc.) for which multiload diagonal generators are subsequently designed. Discussions of the results and criteria for the selection of multiload diagonal generator designs for the three recommended powerplants are presented in Sec. V.

Constant load factors are assumed in the Faraday generator analyses. This simplified approach was taken to ensure that the parametric variations were consistent and to limit the total number of required channel calculations. More sophisticated optimization techniques for Faraday generators[5,6] are not expected to yield different results because the Faraday generator operating characteristics are likely to be altered slightly to accommodate the final multiple diagonal-load designs.

III. Results of Design Sensitivity Analyses

Sensitivities of generator performance to oxygen enrichment level, channel length, Mach number, magnetic field strength, and other factors, were investigated. The results of these sensitivity studies for the three powerplant sizes are discussed in this section. Most extensive parametric variations were performed at the 200 MW_e plant level. These results will be presented first, followed by the results of the 500 and 1000 MW_e plant sizes.

Variation of MHD Generator Performance with Channel Length, Oxygen Enrichment, and Mach Number (200 MW_e Plant Size)

The sensitivity of MHD generator performance to channel length and oxygen enrichment levels was investigated for both subsonic and supersonic channel operations. The Mach number for all subsonic channel designs was 0.885 and the maximum magnetic field intensity was 6 T. For the supersonic channel designs, the peak magnetic field intensity was reduced to 4.5 T and the channel inlet Mach number was 1.2 (with 1.1 and 1.3 as parametric variations).

The enthalpy extraction, η_{EE}, and net MHD efficiency, η_{MHD}, of the subsonic generator designs are shown in Fig. 4 for different oxygen enrichment levels and different channel lengths. The definitions of η_{EE} and η_{MHD} are given in Table 1. The net topping-cycle performance, which is reflected by the values of η_{MHD}, increases with increasing oxygen enrichment and increasing length. However, this increased topping-cycle performance must be weighed against the effects of increased channel heat loss on the steam plant efficiency and the effects of increased sizes of the magnet and oxygen plant on their costs. The corresponding variations in channel heat losses are shown in Fig. 5. Similar to η_{EE} and η_{MHD}, the channel heat losses increase with increasing enrichment and increasing length.

The results of the enthalpy extraction and MHD efficiency for the supersonic generator designs are shown in Fig. 6. In these generator calculations, the internal electrical and gas-dynamic operating parameters were kept within the same prescribed constraints as in the subsonic channel designs. As in the subsonic MHD generators, the values of η_{MHD} increase with increasing enrichment level and increasing channel length. However, the magnitudes of η_{MHD} for supersonic generators, with the lower magnetic fields, were somewhat less than those for the corresponding subsonic designs. The 12-m subsonic generator results are also plotted in Fig. 6 for comparison. The wall heat losses for the supersonic channels are shown in Fig. 7.

The performance of supersonic MHD generators as a function of the channel inlet Mach number was also investigated. The variations of the calculated gross and net MHD power outputs to Mach numbers are shown in Fig. 8. The generator length was 12 m and the oxygen enrichment levels varied from 34 to 36 molar percent oxygen. The net

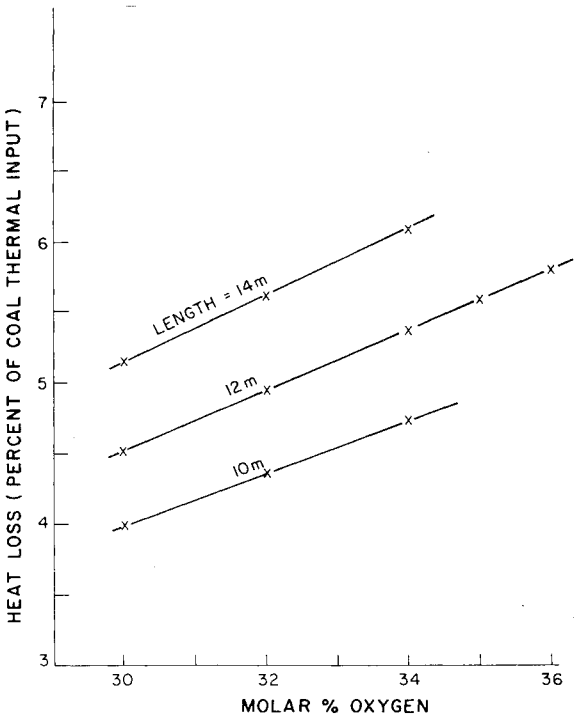

Fig. 5 Variations of channel heat loss with oxygen enrichment and length, 200 MW_e plant sizes, subsonic.

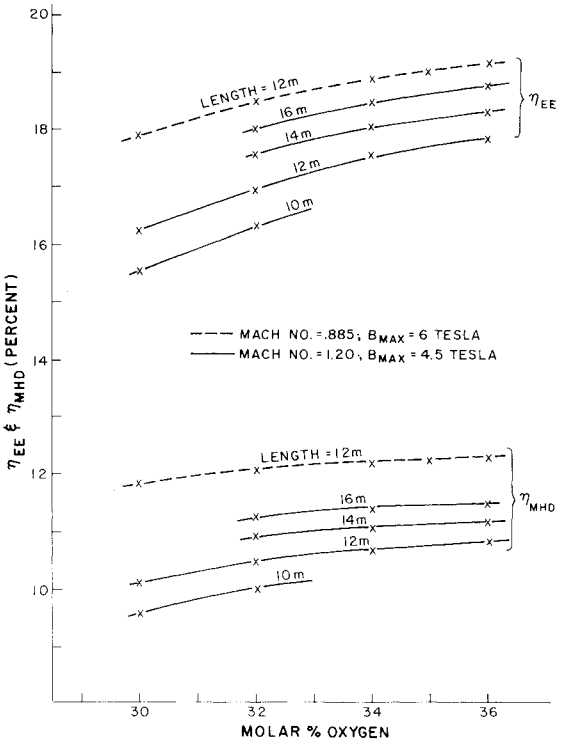

Fig. 6 Variations of η_{EE} and η_{MHD} with oxygen enrichment and length, 200 MW_e plant sizes, supersonic.

power output is not very sensitive to the channel Mach number over the range of values investigated, although the gross power output increases with increasing Mach number. Similar results have been reported in Ref. 6 for the advanced (ECAS scale) MHD powerplants.

The maximum B-field equalled 4.5 T for all of the supersonic channel designs in the present sensitivity analysis. If the B_{max} is allowed to exceed 4.5 T, the performance of those supersonic generator designs at lower Mach numbers (i.e., Mach No. ~1.1) could be improved slightly. Such a trend was

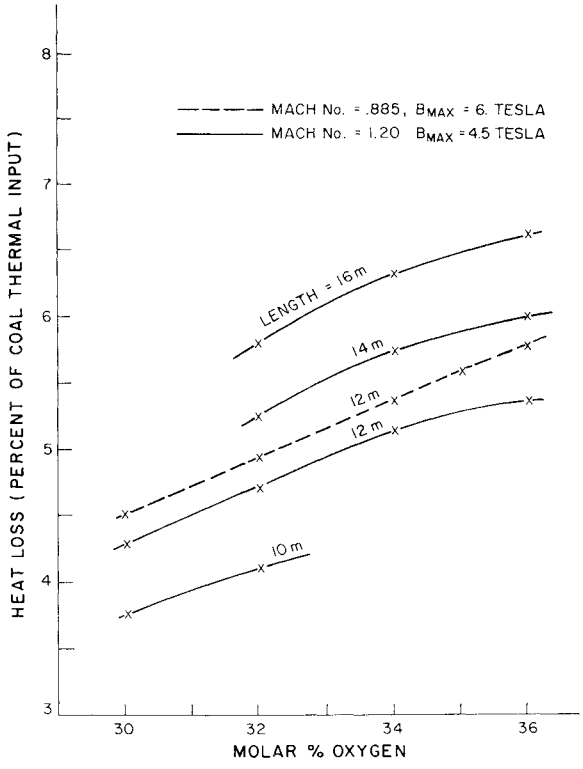

Fig. 7 Variations of channel heat loss with oxygen enrichment and length, 200 MW_e plant sizes, supersonic.

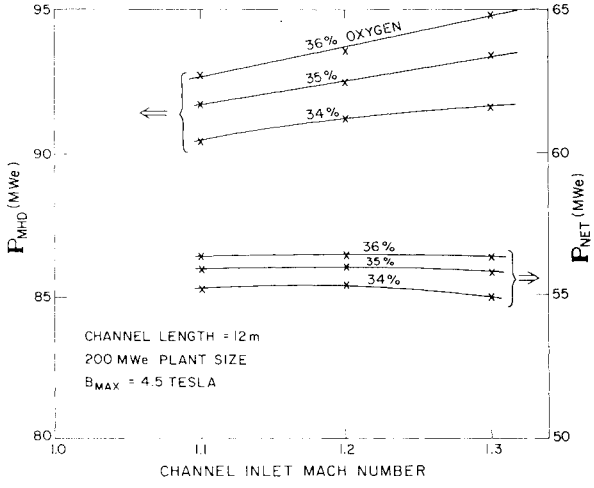

Fig. 8 Variations of gross and net MHD power output for different Mach number and oxygen enrichment.

observed in Ref. 6. However, this slight increase in power output will be accompanied by a corresponding increase in the stored magnetic energy and magnet cost.

Subsonic vs Supersonic MHD Generator Operation (200 MW_e Plant Size)

The selection of the generator Mach number is of great importance because of its strong influence on the overall plant performance and economics and on the design of major powerplant subsystems. Considerations which have influenced the selection between subsonic and supersonic channel operation for the Advanced Power Train study are discussed in this section.

The net MHD power output of a supersonic generator design at 4.5 T peak magnetic field was approximately 10-15% lower than the corresponding subsonic design at 6 T. The resulting difference in the overall net plant efficiency was estimated to be between 0.5 and 1.0 percentage point[1] which

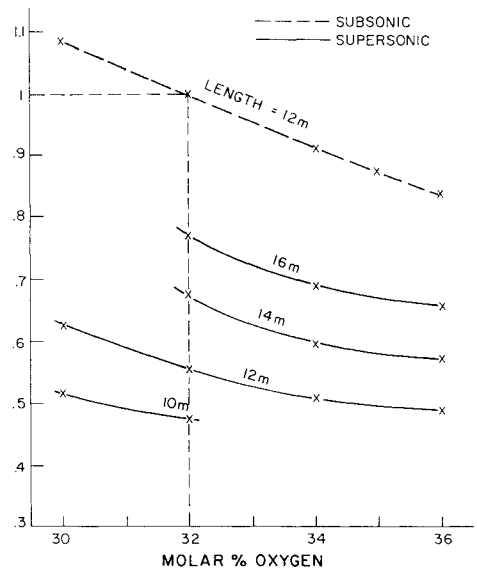

Fig. 9 Magnet stored energy requirement for various oxygen enrichment and length, 200 MW_e plant sizes.

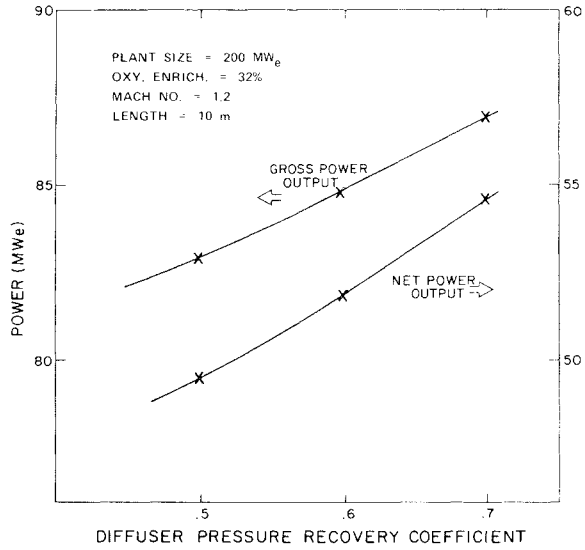

Fig. 11 Variations of gross and net power outputs with diffuser efficiency. 200 MW_e plant size, 32% oxygen enrichment, Mach number = 1.2, length = 10 m.

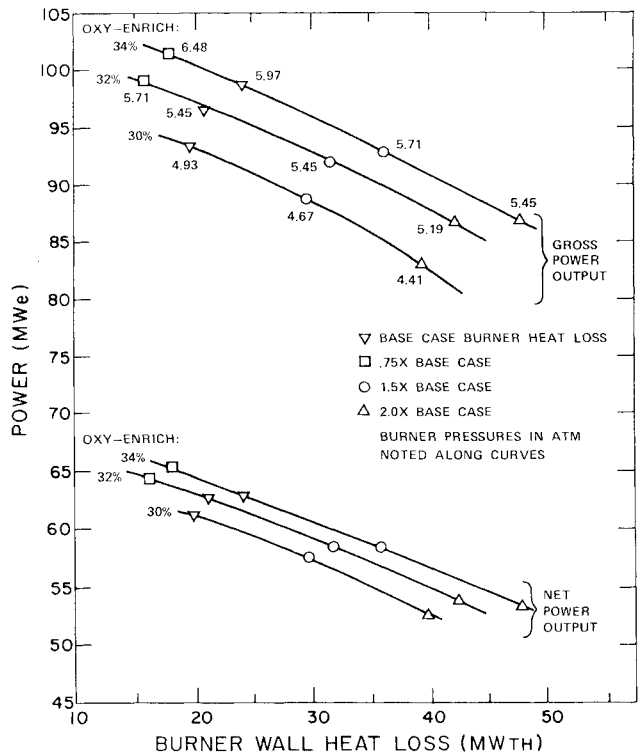

Fig. 10 Gross and net power vs burner wall heat loss for 200 MW_e plant sizes, subsonic.

still resulted in an attractive net plant efficiency for the supersonic generator design. This attractive supersonic MHD generator performance is accomplished with a significant reduction in the stored energy of the magnet. This can be seen in Fig. 9 where the stored energies of the 4.5 T magnets for the supersonic generators are shown for various oxygen enrichment levels and different channel lengths. Comparative data of the stored energies of the 6 T magnets of the 12-m subsonic generators are also shown. The stored energies have all been normalized with respect to one of the subsonic designs (the 32% O_2 channel design). In the case of 32% O_2-enrichment and the 12-m channel, the supersonic generator's magnetic stored energy is only about half of that for the corresponding subsonic design. The lower magnetic energy requirement implies lower magnet cost and risk. As a result of the less costly magnets for the supersonic generator designs, the estimated costs-of-electricity (COE) are practically equivalent for supersonic and subsonic modes of operation.[1]

The supersonic channel has the advantage of not being closely coupled to the burner and, therefore, is less sensitive to burner instabilities than a subsonic generator. In addition, more MHD experience exists to data with supersonic generator operation.

Because of the attractive COE and lesser risks associated with the supersonic channel operation and with the 4.5 T peak magnetic field magnets, this MHD generator design condition was selected for early commercial use.

MHD Generator Performance Sensitivity to Combustor Heat Loss (200 MW_e Plant Size)

The amounts of combustor/nozzle heat loss used in the MHD performance calculations are based on the results of the combustor and nozzle analyses. These latter calculations were carried out as part of the power train component design activities and the results have been reported in Ref. 7. It is difficult to validate the combustor heat loss predictions sufficiently because of the limited available experimental data on MHD coal combustors. For this reason, it was considered important to establish the sensitivity of MHD generator performance to variations in the amount of combustor wall heat loss.

The amount of combustor heat loss was varied from three quarters to twice the basic design value in these sensitivity analyses. Typical results for the variation of gross and net power outputs with assumed heat losses are shown in Fig. 10. The results clearly show the strong dependence of MHD generator performance on the amount of upstream combustor/nozzle heat loss. In order to improve the topping-cycle performance it is essential to minimize these heat losses. The results also show that the pressure ratio across the MHD power train (for maximum P_{net}) decreased with increasing combustor heat loss and decreasing oxygen enrichment.

Sensitivity of MHD Generator Performance to Diffuser Efficiency

The sensitivity of the supersonic generator performance to the diffuser efficiency was investigated by assuming different values for the diffuser pressure recovery coefficient in the comparative channel calculations. The results for gross and net power outputs are shown in Fig. 11. A slightly higher plant operating pressure is desired with the poorer performing diffuser. This causes the slight divergence of the two power

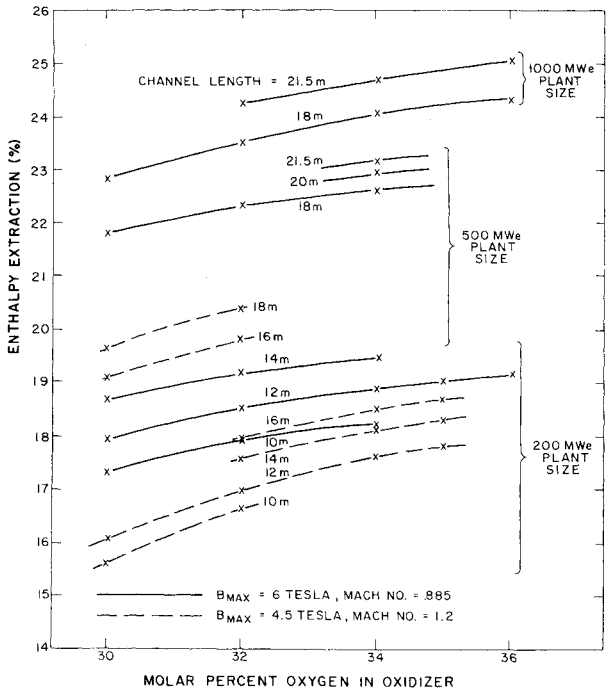

Fig. 12 Enthalpy extraction of MHD generators as a function of oxygen enrichment, channel length, and plant size.

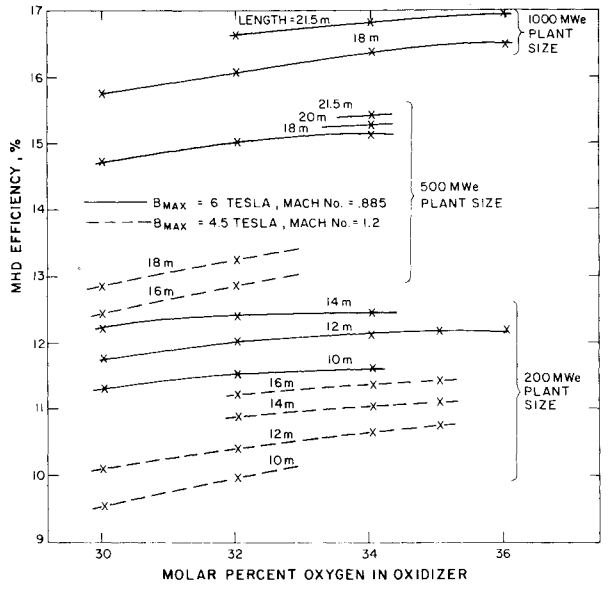

Fig. 13 MHD efficiency of MHD generators as a function of oxygen enrichment, channel length, and plant size.

curves shown in Fig. 11 as the value of C_p is reduced. Similar results have been reported in Ref. 8 for subsonic MHD generator designs.

Generator Performance as a Function of Plant Size

The sensitivity of MHD generator performance to channel length and level of oxygen enrichment was also investigated for the 500 and 1000 MW_e powerplants. For the 500 MW_e plant size, additional generator analyses were conducted to investigate the effects of Mach number and combustor heat loss. The trends exhibited by the results from the analyses of these larger plant sizes are similar to those obtained at the 200 MW_e level.

Supersonic channel operation for the 500 MW_e plant was selected on the same basis as for the 200 MW_e plant: minimum of risk and yet attractive COE. For the large-scale 1000 MW_e plant, emphasis was on maximizing the performance. Risk was not the same prime consideration as for the smaller plants because of the time period over which components can be further developed and experience gained from the smaller plants before such large plants will be constructed. Therefore, only subsonic generator designs at a peak field of 6 T were considered for the 1000 MW_e plant size.

The results of the calculated generator performance for the different plant sizes are compared in Figs. 12 and 13. The calculated enthalpy extractions for the various generator designs are shown in Fig. 12 and the topping-cycle efficiencies are shown in Fig. 13. The figures show the general trend to higher values of η_{EE} and η_{MHD} as the channel thermal input is increased. They also show the decreasing rate at which performance increases as the plant size increases.

The generator performance sensitivity to several channel and powerplant assumptions have been presented in this section. Additional results, such as generator performance dependence on coal types and other factors, can be found in Ref. 9. The final selections of MHD generator design for the three powerplants cannot be based solely on the results of the MHD generator and topping-cycle analyses reported here. Instead, consideration must also be given to overall plant performance, cost, reliability, etc. The discussions of such evaluations are presented in Ref. 1.

IV. Preliminary Results of Part-Load Generator Analysis

Preliminary off-design performance analyses were conducted for the supersonic channel design for the 200 MW_e powerplant. The operating conditions for the MHD generator at 75 and 50% of full-load mass flow rates were established. A summary of the major channel performance data at these part-load conditions is shown in Table 3. The performance data at the nominal full-load condition are also included in the table for comparison.

The magnetic field profile and wall dimensions of the channel used in the part-load analyses are those specified by the design calculations. The heat losses from the combustor including nozzle were estimated to be 79% of nominal load at 75% mass flow rate and 68% of nominal load at 50% mass flow rate. The degree of oxygen enrichment of the oxidizer and seed concentration are the same as at full load, being 32 molar percent O_2 and 1 wt.% K, respectively. It is recognized that the generator's part-load performance could be optimized further by varying these parameters. Such optimization requires additional analyses. It might also be advantageous to increase the oxidizer oxygen content if it proves difficult to maintain the oxidizer preheat temperature at part-load condition.[4] Such powerplant constraints on the part-load operations of the generator will be investigated in the future.

At the ¾-mass flux condition, the generator can operate either in the shock-flow mode or the subsonic mode, depending on the electrical loading. The streamwise variations of flow Mach number for various Faraday load factors are shown in Fig. 14. In the shock mode of operation, the shock will situate somewhere within the first meter of the channel inlet. The exact shock location will depend on the generator loading. As the Faraday load parameter decreases (toward short circuit and higher MHD interaction), the shock will move upstream and eventually the channel will become completely subsonic. In the subsonic mode of channel operation, the burner pressure will increase with increasing MHD interaction.

The variations in the gross and net MHD power outputs and in the burner pressure for different electrical loading are shown in Fig. 15. Channel operation in the shock-flow mode, with shock located at $x \sim 0.6$ m, produced the optimum gross and net power outputs. Consequently this was selected as the operating condition of the generator at ¾-mass flow rate.

At the ½-mass flow rate condition, the generator can

Table 3 Summary of generator off-design performance data for the recommended 200 MW_e plants

	Full load	¾ Part-load	½ part-load
Coal thermal input, MW_{th}	520	390	260
O_2 enrichment, molar %	32	32	32
Mode of operation	Supersonic	Shocked flow	Subsonic
Pressure ratio	5.19	3.90	2.59
Load parameter	0.7109	0.7093	0.7707
P_{MHD}, MW_e	84.85	57.87	30.68
P_{net}, MW_e	51.90	36.36	19.08
Q_{wall}, MW_{th}	21.37	18.07	12.02
Maximum E_{yc}, kV/m	3.81	2.81	2.77
Maximum E_{xc}, kV/m	2.63	1.41	1.11
Maximum J_{yc}, A/cm^2	0.77	0.77	0.58
V_{Hall}, kV	22.3	12.33	6.83
Maximum β	3.94	3.13	3.45
Maximum q_{wall}, W/cm^2	314.0	244.0	174.0
Power density, MW_e/m^3	9.62	6.56	3.48
η_{EE}, %	16.32	14.84	11.80
η_{MHD}, %	9.98	9.32	7.34
η_{isen}, %	60.08	65.19	67.45

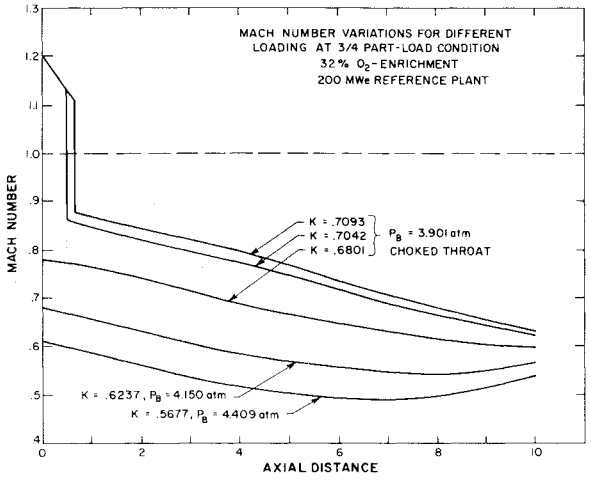

Fig. 14 Mach number variations for different loading at ¾ part-load condition.

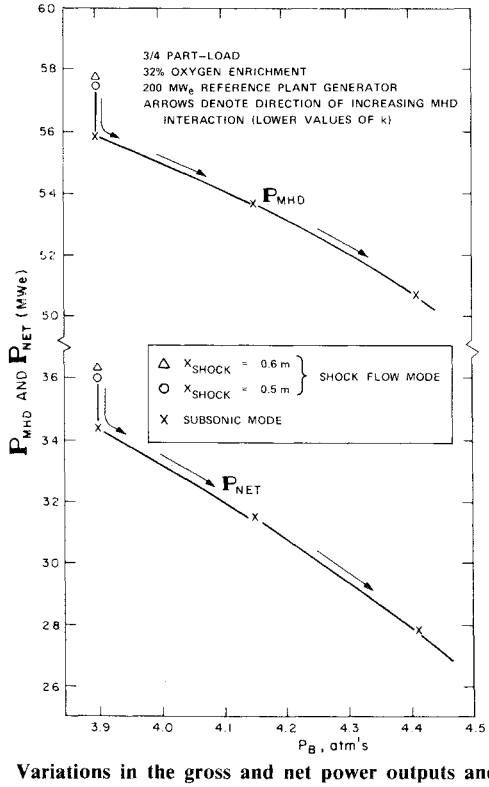

Fig. 15 Variations in the gross and net power outputs and in the burner pressure for different electrical loadings.

operate only in the subsonic mode. The operating condition at this part-load situation was again selected to coincide with the maximum net power output condition.

The results of these off-design studies show that a supersonic MHD generator design can be operated efficiently at part-load conditions. From Table 3 it is seen that the isentropic efficiency is higher at part-load conditions than at full load. This can be explained as follows: The power generated per unit volume and the power dissipated per unit volume are both reduced as the generator mass flux is reduced. However, the dissipated power will be decreasing at a greater rate than the generated power. This is so because the generated power per unit volume is proportional to j while power dissipated is proportional to j^2 and the averaged value of j decreases with decreasing load.

V. Loading and Consolidation Circuitry

Preliminary diagonal-load networks were developed for the MHD generators selected for the three powerplants. A five-terminal load configuration was selected for the 1000 MW_e powerplant, a four-terminal configuration for the 500 MW_e plant, and a three-terminal configuration for the 200 MW_e plant. A schematic of the generator loading network of the 200 MW_e plant is shown in Fig. 16.

Diagonally loaded generator calculations were carried out to aid in the design of the load networks. In these calculations, the wall dimensions of the channels are those specified by the initial Faraday channel design calculations. The number of midchannel power taps, their locations, and the amount of current collected by each tap are determined in the diagonal channel calculations such that the following criteria were satisfied: 1) the local diagonal connecting angle was not excessive, and 2) the current delivered by any midchannel tap was sufficiently low to prevent current nonuniformities from being induced in the plasma. In addition, the generator constraints of Table 2 were not exceeded.

Simpler load connections, with fewer load terminals than those selected here, can also be considered. However, the

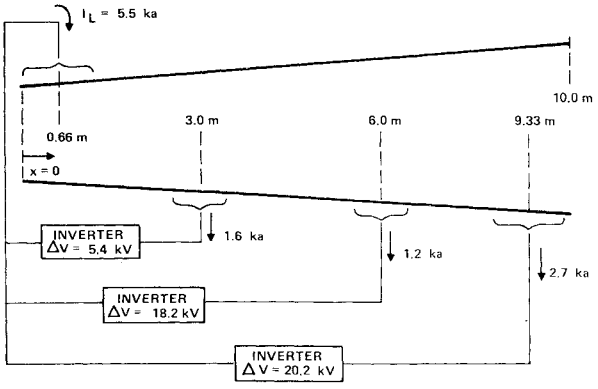

INVERTERS	kV	ka	MW
1ST MID-CHANNEL TAP	5.4	1.6	8.6
2ND MID-CHANNEL TAP	18.2	1.2	21.8
CATHODE TAP	20.2	2.7	54.5
		5.5	84.9

Fig. 16 Three terminal parallel diagonal-load connection for the 200 MW_e plant.

part-load performance characteristics of such simpler loading schemes presently are uncertain. Further investigations are required before a final optimum and practical loading design can be determined for commercial operation.

VI. Summary

Comparative analyses of different MHD generator designs were performed for early commercial MHD powerplant applications. Plant sizes of 200, 500, and 1000 MW_e were considered. The majority of the analyses concentrated on the generator designs for the smallest of these powerplants because it represents a more likely size of the first commercial unit(s). For such first commercial unit(s), minimum of risk and low capital cost were emphasized.

From the analyses it is concluded that a supersonic MHD generator design, operating at a peak magnetic intensity of 4.5 T, is the most attractive for early commercial use. It offers less risk and substantially lower magnet costs compared to subsonic channel operation at a peak magnetic field of 6 T. The penalty in performance of the supersonic generator is relatively small, being on the order of 10-15% less net MHD power output, which corresponds to 0.5-1.0 percentage point less overall powerplant efficiency. This supersonic performance penalty is offset by lower magnet costs, so that the estimated costs-of-electricity are practically equivalent for supersonic and subsonic modes of operation. Subsonic MHD generator operation, with its superior performance, will become more attractive with escalation of fuel costs and as experience is gained with large high field strength superconducting magnets.

The net MHD power output was found to be relatively insensitive to variations in oxygen enrichment levels between 30-34%, and the performance of supersonic MHD generators varied little for variations of Mach numbers between 1.1 and 1.3. Variation in combustor heat loss was found to have a significant impact on MHD generator performance.

Off-design analyses of the supersonic MHD generator design showed that efficient operation can also be obtained at part-load conditions, which is important for practical utility applications. The MHD generator channel operation was found to shift from supersonic to transonic and subsonic operation as the generator mass flux was reduced.

Acknowledgment

This work was supported by the U.S. Department of Energy Under Contract AEPD 81-0004.

References

[1] Muller, D. J. et al., "Definition of a Development Program for an MHD Advanced Power Train—Results from Task I," *Proceedings of the Eighth International Conference on MHD Electrical Power Generation,* Vol. 6, Moscow, Sept. 1983, pp. 114-121.

[2] Gertz, J., Opar, T., Solbes, A., and Weyl, G., "Modeling of MHD Channel Boundary Layers Using an Integral Approach," *Proceedings of the 18th Symposium on Engineering Aspects of MHD,* Paper B. 4 Butte, Mont., June 1979.

[3] Svehla, R. A. and McBride, B. J., "FORTRAN IV Computer Program for Calculation of Thermodynamic and Transport Properties of Complex Chemical Systems," NASA TN D-7056, 1973.

[4] Swallom, D. W., "MHD Channel Performance for Potential Early Commercial Power Plants," *Journal of Energy,* Vol. 7, March-April 1983, pp. 141-146.

[5] Doss, E. et al., "MHD Channel Technical Support for Open-Cycle MHD Program," Argonne National Laboratory, Argonne, Ill., ANL/MHD-78-8, 1978.

[6] Pian, C. C. P., Seikel, G. R., and Smith, J. M., "Performance Optimization of an MHD Generator with Physical Constraints," *Proceedings of the 14th Intersociety Energy Conversion Engineering Conference,* American Chemical Society, Washington, D.C., 1979, pp. 1939-1944.

[7] Hals, F. A., Pian, C.C.P., Demirjian, A.M., Sadovnik, I., and Stankevics, J. O., "Results from Comparative Analysis of Different MHD Generator and Power Train Designs for Early Commercial Power Plant Applications," *Proceedings of the 21st Symposium on Engineering Aspects of MHD,* Paper 1.1.1, Argonne, Ill., June 1983.

[8] "Engineering Test Facility Conceptual Design," Final technical report, Avco Everett Research Lab., Inc., Report No. FE-2614-3, UC-90g, Feb. 1980.

[9] Pian, C. C. P. and Hals, F. A., "MHD Generator Performance Analysis for the Advanced Power Train Study," AIAA Paper 84-0154, Jan. 1984.